Available online at www.sciencedirect.com
SCIENCE DIRECT®
Carbohydrate Polymers 54 (2003) 201–213
Carbohydrate Polymers
www.elsevier.com/locate/carbpol

α-(1–4) Chain distributions of three-dimensional, randomly generated models, amylopectin and mammalian glycogen: comparisons of chromatograms of debranched chains of these polysaccharides and models with random dendrimeric models with the same chain lengths (CL, ICL, ECL) and fractions of A chains

R.A. Caldwell, N.K. Matheson*

Department of Agricultural Chemistry and Soil Science, School of Land, Water and Crop Sciences, The University of Sydney, Sydney, NSW 2006, Australia

Received 18 February 2003; accepted 29 May 2003

Abstract

Previously published chromatographic profiles of amounts of debranched α(1-4) chains versus d.p. of 10 amylopectins (*w*-, *n*- and *ae*-maize, *w*- and *n*-rice, *w*- and *n*-potato and *w*-, *n*- and HA-barley) have been compared with convolved plots of randomly extended and branched, spatially unrestricted models (random dendrimeric) with similar average chain lengths (CL, ECL and ICL) and fractions of A chains: the number of B_k chains in the model was Tb^2a^{k-1} where k is the number of branches. Eight of these comparisons had an undulating, tri-modal pattern of differences (experimental minus model) in the numbers of chains. This was positive at the calculated d.p. of low branched (B_1) chains, negative at medium branched (B_{2-5}) chains and positive at highly branched ($>B_5$) chains. Two gave a bimodal pattern. Plots of glucan versus d.p. emphasised differences at high branching.

Convolved profiles of numbers of types of chains for constructs generated on a three-dimensional cubic grid, in which the positions occupied by chains were exclusive, with extension and branching random—as well as random with a preference for branching into one plane—were compared with spatially unrestricted models with the same average chain lengths and fraction of A chains. Some had a similar undulating tri-modal pattern of differences in chain numbers versus d.p. and these occurred at the same ranges of types of chains to those between debranched amylopectin and the spatially unrestricted models. These differences appeared when the A chain content was equal to or higher than that of amylopectin and were much more marked when the structure of the three-dimensional models was limited along one axis, producing an oblate ellipsoidal shape. These three-dimensional models had more B chains with higher numbers of branches and more chains with longer chain lengths than the spatially unrestricted model with the same number of A chains. In a printout of a two-dimensional construct based on a square grid, with a total of 500 chains (0.58 of which were A chains) a significant proportion of A chains were inside the radius of gyration, and the number of tiers was twice that of the spatially unrestricted model with the same total number of chains and fraction of A chains. The results suggest a model for the distribution between chains with differing numbers of branches in amylopectin, which is affected by steric restrictions. When the A chain content was near to that of mammalian glycogen and expansion not limited along any axis, giving three-dimensional models with a spheroidal shape, the B chain distributions for the three-dimensional and spatially unrestricted models were similar. The resemblance of convolved plots of these to chromatograms of debranched glycogen-also with a spheroidal shape-indicates that its B chain distribution is similar to a randomly generated model in which steric restrictions do not apply.

Keywords: Amylopectin; Glycogen; α-(1–4) glucan chain distribution; Three-dimensional models

1. Introduction

The generation of models of distributions between α-(1–4) chains with different numbers of branches by an algorithm that extended and branched chains by random selection and different probabilities of extension and branching—a randomly generated, dendritic polymer, termed a *random dendrimeric model*—gave constructs in which the numbers of types of B chains were defined by the expression Tb^2a^{k-1}, where k is their number of branches (Matheson & Caldwell, 1999). The construct

* Corresponding author. Tel.: +612-9428-3278; fax: +612-9351-5108.
E-mail address: c.bailey@acss.usyd.edu.au (N.K. Matheson).

0144-8617/03/$ - see front matter © 2003 Elsevier Ltd. All rights reserved.
doi:10.1016/S0144-8617(03)00161-9

Nomenclature

a	fraction of A chains
b	fraction of B chains
β	fraction of glucosyl residues removed by β-amylolysis
B_A	probability of branching an A chain
B_B	probability of branching a B chain
CCL	average core chain length (glucosyl units)
CL	average chain length of A + B chains
CL_A	average chain length of A chains
CL_B	average chain length of B chains
CL_S	average number of glucosyl units in segments of B chains between branches (including one branching residue in each segment of the α(1–4) chain) plus the A and external B chains
d.p.	degree of polymerisation (glucosyl units)
DP	mean degree of polymerisation of a population of a particular type of chain, such as A, B_1,…
3D(P)	three-dimensional model with preferential branching
3D(R)	three-dimensional model with random branching
E_A	probability of extension of an A chain
E_B	probability of extension of a B chain
ECL	average external chain length
ECL_B	average chain length of segments of B chains external to the outermost branch point
F	average frequency of branching
$G_{x,y,z}$	radii of gyration
ICL	average internal chain length
IEC	ion-exchange chromatography
M_S	molecular size
M_W	molecular weight
N	value of the highest tier number
PAD	pulsed amperometric detection
R(SU)	spatially unrestricted randomly constructed model (random dendrimeric)
SEC	size exclusion chromatography
T	number of chains per molecule
w	range of d.p. at half height of the distribution of a population of a particular chain type

applies no spatial restrictions to the placement of new chains. Different types of chains (A, B_1, B_2, etc.) can be generated in any tier. However, the termination of the process and the dependence of the formation of chains with higher levels of branching on the prior existence of chains with fewer branches precludes a fully random, final arrangement of the various types of chains. This is non-regular. Calculation of DP values for the A and the various types of B chains from the generally accepted a, ECL and ICL values, and convolving these, gave profiles of numbers of chains or amount of glucan versus d.p. Comparison with available experimental chain profiles (to about a d.p. of 60) of debranched mammalian glycogen showed that this model gave a much better fit to the experimental data of proportions of debranched α(1–4) chains versus d.p. than a model with regular branching of B chains with two—and some single—chains. However, amylopectin, although showing much similarity, had a major difference: comparison of plots of weight of glucan at a $d.p_n$ versus $d.p_n$ showed that, in contrast to the model, experimental chromatographic profiles had another peak at long chain lengths. The introduction of post-column depolymerisation of the α(1–4) chains from debranching, by hydrolysis to glucose with amyloglucosidase (Wong & Jane, 1997) has overcome any problems of differential detector response to PAD of α(1–4) glucan chains with differing d.p. These authors have examined a range of amylopectins (Jane et al., 1999; McPherson & Jane, 1999; Song & Jane, 2000).

We have now compared the chromatographic profiles of amount of glucan and numbers of chains versus d.p. to those of the R(SU) models (called random dendrimeric in Matheson et al. (1999)) derived from the chain lengths (CL, ECL, CCL and ICL) determined for 10 of the experimental chromatograms. Models have also been generated with two programs in which chains are located on a three-dimensional cubic grid. The events (extension or branching of A or B chains) were chosen randomly. The positions on the grid are unique; two chains cannot occupy the same space. In one program, if branching was selected, the direction of the new branch was chosen—subject to the spatial restrictions—in sequence on a preferential basis. In the other, the direction of the new branch was chosen randomly. These two models have been compared with the R(SU)model and the differences related to those found between the experimental profiles and the R(SU) model.

2. Methods

2.1. Construction of convolved R(SU) profiles

Average chain lengths (CL) were calculated from published experimental chromatographic profiles (Jane et al., 1999; McPherson et al., 1999; Song et al., 2000) of amount of glucan in a chain of $d.p_n$ as

$$CL = \frac{\sum_{n=1}^{n} \text{detector response of chain of } d.p_n}{\sum_{n=1}^{n} \frac{\text{detector response of chain of } d.p_n}{d.p_n}}$$

where the unit is number of glucosyl units.

Then

$$\beta\mathrm{CL} = a(\mathrm{CL_A} - 2.5) + b(\mathrm{ECL_B} - 1.5)$$

$$= a\mathrm{CL_A} + b\mathrm{ECL_B} - 2.5a - 1.5(1 - a)$$

and

$$\mathrm{ECL} = \beta\mathrm{CL} + a + 1.5 = \beta^{*}\mathrm{CL} - b + 2.5$$

and

$$\mathrm{CCL} = (\mathrm{CL} - \mathrm{ECL} - b)/b \text{ and ICL}$$

$$= b\mathrm{CCL} - a \text{ (Yun\&Matheson, 1993)}$$

For calculation of DP, $\mathrm{CL_A}$ and $\mathrm{ECL_B}$ were taken as equal, β as 0.56, and the DP of B_k as $\mathrm{ECL} + k(\mathrm{ICL} + 1)$. The average numbers of chains of a B type were calculated as Tb^2a^{k-1} and the numbers of A chains as Ta ($T = 1260$). Gaussian distributions for each type of chain (based on its DP) were convolved with Microcal Origin® software (Matheson et al., 1999). The w values for B chains were 6 for w--rice, 8 for amylomaize V and 7 for all other amylopectins. The A chains were convolved as skew curves from two populations of 220 and 486 chains. Their DP values and w values (in brackets) were; w-rice 8.5 (3) and 11.5 (4); w-maize 10.7 (4) and 12.7 (6); w-barley 10.5 (4) and 12.5(6); w-potato 11.0 (4) and 13.0 (6); n-rice 10.5 (4) and 12.5(6); n-maize 10.8 (4) and 12.8 (6); n-barley 11.2 (4) and 13.2 (6); n-potato 11.6 (4) and 14.1 (6); amylomaize V 12.5 (5) and 14.5 (7); HA barley 11.2 (4) and 13.2 (6).

2.2. Algorithm for the generation of a spatially limited model

The algorithm developed for the three-dimensional models follows the conformational requirements for either extension or branching of a randomly branched dendrimer [R(SU)] as outlined in program 1, which appeared in a previous publication (Matheson et al., 1999) together with spatial restrictions placed upon the growing construct. In summary these consist of a *pre-event configuration* and *status value*, the *event*, and a *post-event configuration* and *status value*. The possible events are extension of an A chain, extension of a B chain, branching of an A chain, and branching of a B chain. Each event can be assigned a probability (E_A, E_B, B_A, and B_B, respectively). The program commences with a linear three-link segment and terminates when a pre-assigned number of chains (T) have been generated (≤ 1260). In the 3D(R) and 3D(P) programs the constructs are generated in a cubic grid with the spatial restrictions preventing chains from extending or branching into coordinates already occupied. Two further controls may be placed on the growing three-dimensional construct, namely a radial limit in the X–Y plane and a limit of growth in the Z direction. In both programs the radial limit in the X–Y plane is set at 60 grid units whilst, the limit of growth along the Z-axis is either + 60 to − 60 or + 3 to − 3 grid units. The permitted range of coordinates is therefore cylindrical with the centre of mass of the cylinder at $x, y, z = 0$. The initial linear three-linked segment occupies co-ordinates from $x, y, z = 0$ to $x = 3$ and y and $z = 0$ grid units. In the 3D(P) program, after a chain and event are chosen randomly, if the event is branching the direction to be occupied by the new chain is chosen in a preferential sequence as shown in Table 1. If the selected space is already occupied, the next direction in the sequence is examined. In the 3D(R) program the chain and the event are chosen randomly but, if the event is branching, the direction of the new chain is also chosen randomly. If the selected position is already occupied, the event is voided and a new chain and event chosen randomly. The program re-commences for a pre-set number of repeats (normally set at an additional 7) with the same input values. On completion of the program the following information is presented:

Table 1
Sequence of branching choices in the 3D(P) model

Axis and direction of chain undergoing branching	Sequence of possible axes and directions for the new branch
X + ve	Into Y + ve then Y − ve, Z + ve and Z − ve
Y + ve	Into X − ve then X + ve, Z + ve and Z − ve
Z + ve	Into X − ve then X + ve, Y + ve and Y − ve
X − ve	Into Y − ve then Y + ve, Z + ve and Z − ve
Y − ve	Into X + ve then X − ve, Z + ve and Z − ve
Z − ve	Into Y + ve then Y − ve, Z + ve and Z − ve

1. the average number of A chains
2. the average number of chains with specific chain lengths
3. the average number of B chains with a specific number of branch points
4. the average number of links (equated to a degree of polymerisation) in the construct generated for a pre-set number of chains and probabilities
5. the average number of links in the A chains
6. the average number of links between branch points of the B chains
7. the moments of inertia and radii of gyration about each axis for each repeat
8. the centre of mass of the generated construct for each repeat

Standard deviations of the eight repeat replicates were also provided. Radii (x, y, z) of the ellipsoid were estimated with Routh's rule from the average radii of gyration ($G_{x,y,z}$) assuming a symmetrical shape with uniform density (Bullen, 1962) as:

$$x = 2.5\sqrt{G_y^2 + G_z^2 - G_x^2}$$

Similar expressions apply for y and z. The axial ratio is $(x + y)/2z$.

3. Results and discussion

3.1. Comparison of experimental profiles with R(SU) models

The CL values (Table 2) of 10 amylopectins were derived from their chromatographic profiles (Jane et al., 1999; McPherson et al., 1999; Song et al., 2000). The average chain length is the total number of glucosyl residues divided by the total number of chains, that is:

$$\frac{\sum_{n=1}^{n} \text{number of Glc residues in a chain of d.p}_n}{\sum_{n=1}^{n} \text{number of chains of d.p}_n}$$

where n is the longest chain.Since the 'number of Glc residues in a chain of d.p$_n$ × number of chains of d.p$_n$' equals the amount of glucan in chains of d.p$_n$, the first expression is equivalent to:

$$\frac{\sum_{n=1}^{n} \text{detector response of chain of d.p}_n}{\sum_{n=1}^{n} \dfrac{\text{detector response of chain of d.p}_n}{\text{d.p}_n}}$$

To make profiles of the models, DP values of B chains with the various numbers of branches were calculated (Section 2.1) from the ECL, CCL, and ICL values (Table 2). Combined with the numbers of each type of chain, these were convolved to give a profile of relative numbers of chains per 1260 residues versus d.p. These were normalised to a total of 1000 chains. Amount of glucan of d.p$_n$ was then calculated by multiplying by d.p. and the values normalised to 1000 to give a profile of relative amount of glucan of d.p$_n$ versus d.p. Experimental chromatographic profiles of amount of glucan versus d.p$_n$—of four waxy, four normal and two high-amylose samples—were converted to numbers of chains of d.p$_n$ by dividing by d.p$_n$, and normalising to a total of 1000 chains. Of the four waxy samples considered, apparent amylose contents (from I_2 absorption) of rice and maize were zero (Jane et al., 1999), whereas those of barley and potato were 9.1 and 19.2 (Song et al., 2000). In the experimental chromatographic profiles there are some differences in the various chain lengths (CL, ECL, CCL and ICL) among the amylopectins; in particular *w*-rice compared to *n*-rice and to all other samples, as well as amylomaize V to *n*-maize and to the other structures.

Table 2
Average chain length values of amylopectins calculated from experimental chromatograms (numbers of glucosyl units)

Amylopectin	CL	ECL	CCL	ICL	d.p. of longest chain in experimental profile	d.p. of B_{10} chain in model
w-Maize	18.3	12.1	13.1	5.2	73	74
w-Rice	15.5	10.6	10.1	3.9	66	60
w-Potato	18.8	12.4	13.6	5.4	86	76
w-Barley	17.8	11.9	12.6	5.0	67	72
n-Maize	18.4	12.2	13.1	5.2	80	74
n-Rice	17.8	11.9	12.5	5.0	80	72
n-Potato	20.4	13.3	15.2	6.1	85	84
n-Barley	19.2	12.6	13.9	5.6	83	79
ae-Maize	21.6	13.9	16.4	6.6	86	90
HA-barley	19.1	12.6	13.9	5.5	77	79

The experimental samples were prepared by the removal of molecules with long α(1–4) chains as the *n*-butanol complexes (Jane et al., 1999; McPherson et al., 1999; Song et al., 2000). Estimation of A_{max} and λ_{max} values of the iodine complexes across the chromatographic profiles obtained by SEC of starches (Baba & Arai, 1984; Baba, Uemura, Hiroto, & Arai, l987A,B; Boyer, Damewood, & Matters, 1980; Ebermann & Schwarz, 1975; Gérard, Barron, Colonna, & Planchot, 2001; Yamada & Taki, 1976; Yeh, Garwood, & Shannon, 1981) and fractions of starches (Baba & Arai, 1984; Matheson, 1971, 1990, 1996; Klucinec & Thompson, 1998; Matheson and Welsh, 1988; Yamada and Taki, I976; Yun and Matheson, 1992, 1993) indicates that starch consists of a continuum of structures, present in differing proportions according to genotype. The spectrum of structures ranges continuously from highly branched molecules of high molecular size in which CL_S is short, and which have low A_{max} and λ_{max} values of their iodine complexes, to those of lower molecular size with increasing CL_S and which have higher λ_{max} and A_{max} values of their I_2 complexes. The patterns of amounts of these structures detected on SEC varies among genotypes. Waxy maize is essentially devoid of material of low M_S and high CL_S, *n*-maize has a region of low frequency of occurrence between the material of high M_S with short CL_S and of low M_S with very long CL_S (amylose): *ae*-maize has higher amounts in this intermediate region. Extracts of phytoglycogen from su_1 maize can be separated by increasing centrifugal force into fractions with progressively lower M_S, CL and amounts of polymer with a high CL_S that forms I_2 complexes characteristic of amylose (Matheson, 1975). For a branched structure in which T is large the average number of glucosyl units in segments of B chains between branches (including the branching residues in the α(1–4) chains) plus the A and external B chains (CL_S) approximates CL/2 (Burchard & Thurn, 1985). CL_S equals the total number of glucosyl units/total number of segments, namely

$$T \times \text{CL}/[Ta + Tb(F+1)] = \text{CL}/(1+bF)$$

and since $F \rightarrow 1/b$ when T is large $CL_S \approx 1/2CL$

The total number of segments is $2T - 1$.

The nature of the fraction isolated as amylopectin depends on the method of fractionation and the conditions used; for example, the centrifugal force sedimenting a complex, or the point of division on chromatography. Chain length values differ according to the fractionation procedure. SEC and ultracentrifugation depend on M_S, complexation with alcohols (such as *n*-butanol) on CL_S, and in concanavalin A complexation, degree of branching and M_S are factors. The different methods separate broadly into two fractions but points of division vary. The precipitate from complexation with *n*-butanol, when

examined by SEC shows material of high M_S with low λ_{max} and A_{max} values (Baba et al., 1987A,B; Matheson, 1971, 1990; Matheson et al., 1988; Oates, 1990; Takeda, Hizukuri, & Juliano, 1986; Yamada et al., 1976). Different alcohols give different amounts of complex (Greenwood & Robertson, 1954; Klingler & Zimbalski, 1992; Klucince et al., 1998; Whistler & Doane, 1961). *n*-butanol interacts with longer uninterrupted α(1–4) sections than thymol and so precipitates more material of higher M_S as amylose. As SEC does not give baseline separation, fractionation is incomplete (Gérard et al., 2001). Concanavalin A gives more material as amylopectin than does *n*-butanol, as it complexes with some branched polymer with longer α(1–4) chains. Consequences are that branched fractions prepared by *n*-butanol complexation of different starches have less product with longer branches, showing greater similarity in structural properties (CL, ECL, CCL and ICL) among one another than is found among those prepared by complexation with concanavalin A or by SEC: an amylopectin fraction is defined operationally, according to the method of fractionation.

The experimental chromatographic profiles of debranched amylopectins obtained by Jane et al. (1999), Song et al. (2000), and McPherson et al. (1999) re-plotted as relative numbers of α(1–4) chains versus d.p., have been compared with the distribution of relative numbers of chains in models convolved from the chain-length values (ECL and ICL-Table 2) derived from the experimental graphs and the numbers of chain types calculated for the R(SU) model. Fig. 1 shows difference plots for *w*-, *n*- and *ae*-maize, *w*- and *n*-rice and *w*-potato. Table 3 gives numerical data for the differences in numbers of chain types for all 10 amylopectins and compares other data of their profiles.

Since the amount of glucan at $d.p_n/d.p_n$ = the number of chains at $d.p_n$, plots of amount of glucan at $d.p_n$ versus d.p.—a common method of reporting experimental profiles—accentuate differences at high α(1–4) chain-lengths relative to those at short chain-lengths. Conversely, plots of numbers of chains versus d.p. emphasise differences at low d.p. relative to high d.p. This is shown in Fig. 2A and B, where plots of amounts of glucan and numbers of chains of the experimental profiles of debranched *n*-potato amylopectin are compared with the convolved R(SU) model. When plotted as weight of glucan versus d.p., the experimental curves had a second peak or point of inflection (*w*-rice, *w*-barley, *n*-barley and HA-barley) at a d.p., that corresponded approximately to the d.p. of B_5–B_6 chains. When plotted as number of chains versus d.p., this peak was reduced to a plateau or a diminished rate of decrease for *w*-rice, *w*-barley, *w*-barley, and *w*-maize, and a much reduced size of peak for *w*-potato *n*-rice, *n*-maize, *n*-potato and *ae*-maize.

The experimental chromatograms and the convolved profiles of models of the same genotype have a number of resemblances (Table 3). The d.p. values of their maxima are similar, as also are the mean d.p. values of the 560 chains of lowest d.p., as well as the d.p. of the chain numbered 560 (starting from the shortest chain): an *a* value of 0.56 gives 560 A chains per 1000 chains. In amylopectin, due to the high number of A chains, the maximum in the chromatographic profile of numbers of debranched chains versus d.p. can be expected to be due largely to A chains. The coincidence of the d.p. of the experimental maximum and the ECL calculated from CL, β and *a* of the experimental profiles, and the correspondence of this peak to those in the models—where CL_A, ECL_B and ECL have been set equal—indicates that in these amylopectins $CL_A \approx$ ECL and hence $ECL_B \approx CL_A$.

A feature of the experimental profiles of the amylopectins is an excess of numbers of B chains of d.p. of approximately 14–24 (except *n*- and *w*-barley) over those in the convolved model, a shortfall at intermediate values of d.p. 25–42 and another excess at d.p. values of more than 42 (high d.p.). From the calculated DP of B chains, there is an excess of B_1 chains (low branching), a shortfall in the region of B_2, B_3, B_4 and B_5 chains (medium branching) and another excess at the d.p. values of chains with more than five branches (high branching). An undulating pattern of differences was found by Hanashiro, Abe, and Hizukuri, (1996)when chromatograms of the amount of glucan at different d.p. values of debranched chains of a number of amylopectins were compared to arrowhead amylopectin. A peak at high chain lengths has been described for both SEC and IEC-PAD profiles (Gunja-Smith, Marshall, Mercier, Smith, & Whelan, 1970; Hanashiro et al., 1996; Jane et al., 1999; MacGregor & Morgan, 1984; Manners, 1989; Shibanuma, Takeda, & Hizukuri, 1996) and also for electrophoresis of fluorescently labelled chains (O'Shea & Morell, 1996). In *w*-rice (Fig. 1, Table 3) this peak was just detectable and the difference from the model very small (1 chain in 1000). The maximum difference was found in *n*-potato (35 chains per 1000—Table 3 and Fig. 2A and B). In general, the differences in the numbers of long chains were less than for both short and medium chains in the same polymer.

3.2. Generation of spatially restricted three-dimensional models

From the physico-chemical data of amylopectin it was proposed (Banks, Geddes, Greenwood, & Jones, 1972; Kerr, 1945) that its behaviour in aqueous solution was consistent with it being a flat molecule—a two-dimensional entity—and that this structure was a consequence of the method of synthesis in the plastid. A wide range of M_w values (approximately $1–600 \times 10^6$) has been reported for amylopectin solubilised by different procedures from various sources (Ahmad, Williams, Doublier, Durand and Buleon, 1999; Durrani & Donald, 2000; Millard, Wolf, Dintzis, & Willett, 1999; Thorn & Mohazzeb, 1990). Estimation is difficult because of the tendency for aggregation in solution and the dependence of sedimentation on concentration

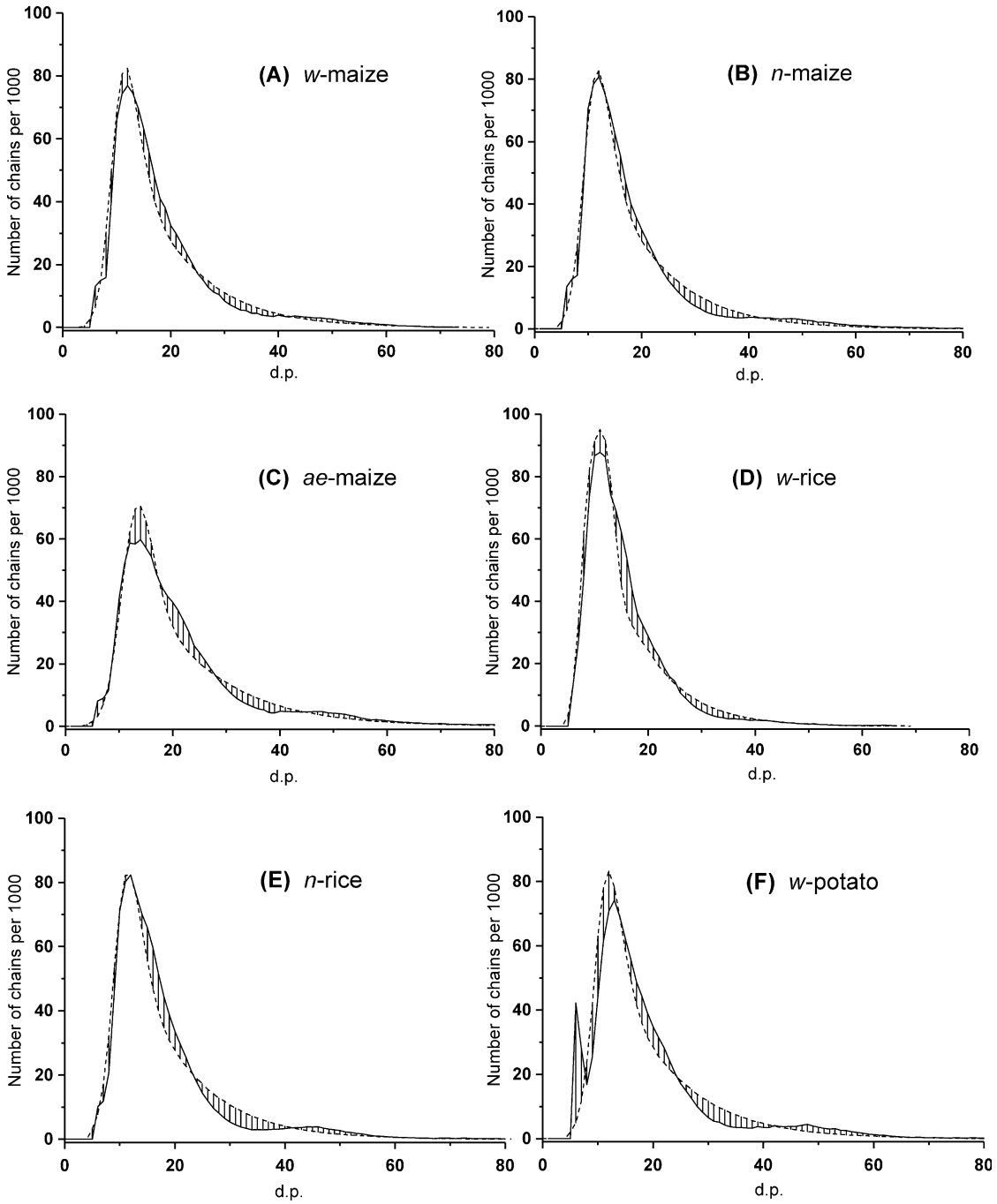

Fig. 1. Comparisons of the experimental chromatographic profiles of α(1–4) chains of debranched amylopectin with the convolved profiles of the R(SU) models with the same *a*, CL, ICL and ECL values. (- - -) R(SU) model; (—)experimental chromatogram.

during ultracentrifugation (Bryce, Cowie, & Greenwood, 1957; Durrani et al., 2000). Molecules of a wide range of sizes are present. Examination of amylopectin from wheat grains by ultracentrifugation and pulsed-field gradient n.m.r. in DMSO (Lelievre, Lewis, & Marsden, 1986; Callaghan & Lelievre, 1985) indicated a M_w of 0.4–2×10^6 in this solvent, and a disc-like shape (oblate ellipsoid) with an axial ratio of about 38 by ultracentrifugation and 18 by pulsed-field gradient n.m.r. The β-limit dextrin had a reduced (but still high) axial ratio, ~5, (Callaghan, Lelievre, & Lewis, 1987) indicating that the external chains lie in the plane of the long axes of the parent amylopectin and that the core chains also have an oblate ellipsoidal structure. The disc-shaped amylopectin molecules were considered not to aggregate in the 'good' solvent DMSO, whereas in water (which is a less 'good' solvent) to aggregate to a less planar assembly with a volume up to about 400 times that of individual molecules. Small-angle X-ray scattering with synchroton radiation gave strong evidence that amylopectin is a non-spherical

Table 3
Comparison of chain length data of debranched chains in experimental (**E**) chromatograms with the R(SU) model (**M**) (expressed as number of glucosyl residues)

Amylo-pectin	Type of data	CL of 560 chains of lowest d.p.	d.p. of chain 560	d.p. of high peak and number of chains (in brackets)	Difference in number of chains (**E** − **M**) and range of d.p. (in brackets)		
					Low branching	Medium branching	High branching
w-Maize	**E**	12.1	16	12(77)	+57	−30	+11
	M	11.6	16	12(82)	(14–24)	(25–42)	(43–67)
w-Rice	**E**	10.8	14	11(74)	+84	−26	+1
	M	10.3	14	11(79)	(14–25)	(26–40)	(41–66)
w-Potato	**E**	12.0	17	13(74)	+54	−54	+43
	M	12.1	16	12(83)	(14–24)	(25–41)	(42–86)
w-Barley	**E**	11.3	15	11(92)	−12	−36	+21
	M	10.9	16	11(82)	(13–22)	(23–43)	(44–67)
n-Maize	**E**	11.9	16	12(53)	+37	−48	+19
	M	11.9	16	12(54)	(14–22)	(32–42)	(43–80)
n-Rice	**E**	11.9	16	12(82)	+71	−59	+16
	M	11.6	16	12(82)	(12–23)	(24–41)	(42–79)
n-Potato	**E**	12.4	18	13(67)	+18	−60	+35
	M	13.1	18	13(78)	(17–24)	(25–44)	(45–85)
n-Barley	**E**	11.8	16	11(84)	−28	−39	+24
	M	11.6	17	12(82)	(14–22)	(23–43)	(44–83)
ae-Maize	**E**	13.7	19	14(60)	+49	−36	+16
	M	13.5	19	14(70)	(18–27)	(28–45)	(45–86)
HA-barley	**E**	12.2	17	12(84)	+15	−34	+14
	M	12.3	17	12(82)	(15–24)	(25–43)	(44–77)

macromolecule in both water and DMSO (Durrani et al., 2000). The high viscosity of amylopectin and the large decrease in elution volume on SEC after periodate oxidation followed by borohydride reduction (with opening of the pyranose ring) of the β-limit dextrin (Tao & Matheson, 1993) are also consistent with a flat structure. Its behaviour contrasts with that of glycogen, whose properties in solution indicate a spherical molecule (Banks et al., 1972; Bryce et al., 1957; Callaghan & Lelievre, 1986; Larner, Ray, & Crandall, 1956; Madsen & Cori, 1958; Tao et al., 1993). The sedimentation constant of glycogen shows slight or nil concentration dependence, the solution viscosity is approximately one order of magnitude lower than for amylopectin, the limiting viscosity number is virtually independent of solvent and its β-limit dextrin gives no significant change in elution volume on SEC after oxidation with periodate and reduction with borohydride.

From the products of partial hydrolysis by acid (Gérard, Colonna, Buleon, & Planchot, 2002; Robin, Mercier, Charbonniere, & Guilbot, 1974) or α-amylase (Bertoft, 1989; Bertoft & Koch, 2000) and the physico-chemical properties, the currently accepted arrangement of chains in amylopectin (Manners, 1989; Thompson, 2000) is the cluster model. The various two-dimensional, partial representations of this model show differences. In some, the α(1–4) chains linking the cluster-units have

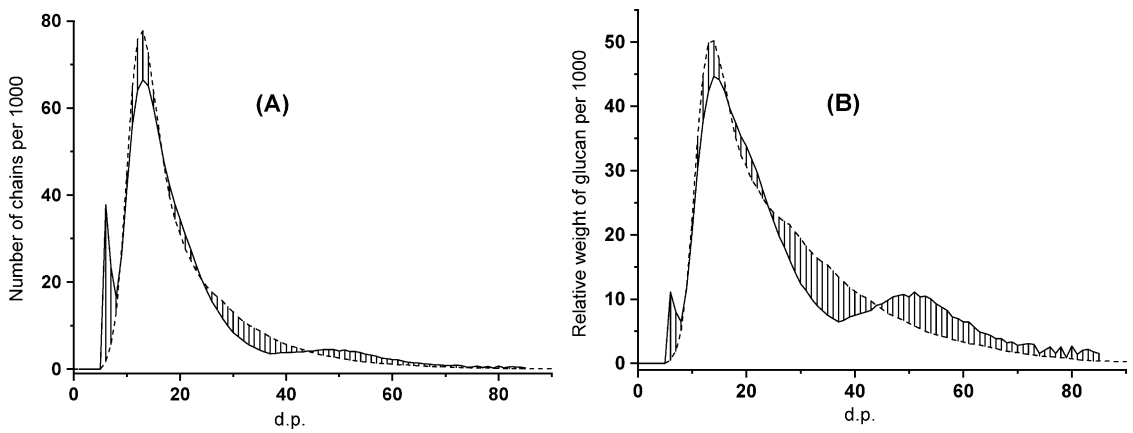

Fig. 2. Comparisons of differences between numbers of α(1–4) chains (A) and weight of glucan (B) versus d.p. of the experimental profile of *n*-potato amylopectin (—) and the convolved profile of the R(SU) model (- - -) with the same CL, ICL, ECL ($ECL_{B=}CL_{A)}$ and *a* value.

relatively long sections free of any α(1–6) linked branches (French, 1984; Nikuni, 1978) in others these longer linking chains have α(1–6) branches attached (Hizukuri, 1986; Robin, et al., 1974) with a significant proportion of A chains in the interior sections of the molecule (Manners & Matheson, 1981). The longer α(1–4) chains linking cluster-units may arise non-regularly from any tier within a cluster-unit in the lower stratum (Manners et al., 1981) or they may be predominantly an extension of the zero tier (the single basal chain)in the cluster-unit in this lower stratum (French, 1984; Hizukuri, 1986). Hence, differences among the models include the proportions of cluster-units with different numbers of links to other cluster-units and the tier pattern (including the basal tier of the unit) from which other cluster-units arise. At present it is not possible to establish which particular pattern occurs.

The program for the R(SU) model (Matheson et al., 1999) is spatially unrestricted. To determine the effects of spatial restriction, models have been developed on two-dimensional square and three-dimensional cubic grids, in which the position occupied by each chain is exclusive. Fig. 3 is the output of a single random construct on a two-dimensional square grid with $E_B = 0.60$, $(E_A = 1 - E_B)$ B_A and $B_B = 2$ and $T = 500$. The a value is higher than for the R(SU) model with the same probabilities (0.58 compared to 0.55) and there are 10% more B_1 chains than in the R(SU) model with the same a value (0.58).The dotted circle shows the radius of gyration: a mean of three replicates was 16 grid units. A chains are found in the interior; with 32% lying inside the radius of gyration. Further extension or branching of some chains is limited by the presence of neighbouring chains: development of some is sterically restricted. The numbers of α-(1–4) chains of various lengths are somewhat similar in both models (Table 4) but there are major differences in the tier structures. The two-dimensional model has many more tiers. Whereas N was nine in the R(SU) model it was 20 in the two-dimensional construct. Thirty percent of its tiers were in those numbered >9. The single basal chain is numbered as 0. A chains were spread over all tiers with 65% connected to tiers 1–9.

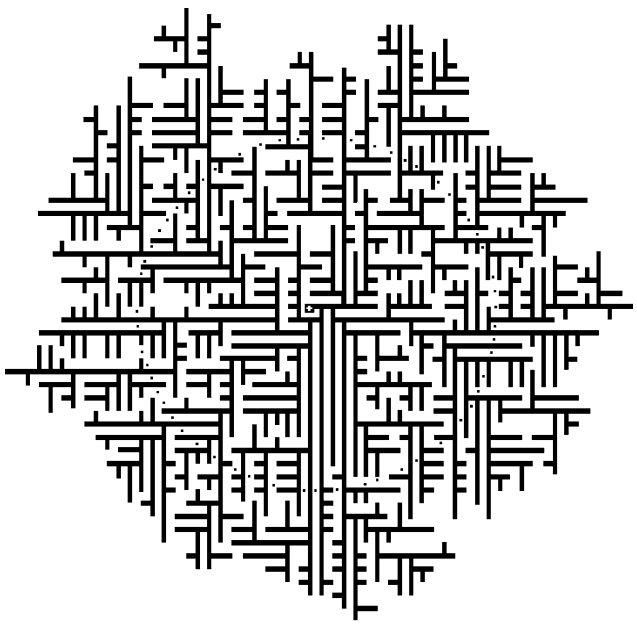

Fig. 3. Printout of a two-dimensional construction of a model, randomly generated on a square grid ($a = 0.58$).

Table 4
Comparison of properties of a R(SU) and a two-dimensional randomly generated construct ($T = 500$) with the same a value (0.58)

Property	Model	
	R(SU)	2D(R)
E_B	0.65	0.60
Lengths of chains (grid units)		
Mean	2.8	3.0
Mode	1	1
Median	1.5	1.6
no. > 14	1	7
Tier structure (no.)		
Mean	4.4	8.8
Mode	4	8
Median	3.9	7.8
N	9	20

In one of the three-dimensional cubic models [3D(P)] the direction of branching from each axis was determined on a preferential basis that included all possibilities. However, preference was given to branching into one plane, the X–Y. Some possible directional influences in the biosynthesis of amylopectin are the chirality of D-glucose and the synthesizing enzymes, the formation of helices by the α(1–4)-glucan chains and the tendency for sections of these to bind to each other. There is also limited extension into the short axis due to the oblate ellipsoidal shape. In the 3D(R) model, the direction of branching was chosen randomly.

3.3. Comparison of three-dimensional with their R(SU) models

From the a values of the three-dimensional models the numbers of B_k chains (Tb^2a^{k-1}) were calculated for the R(SU) model with the same a value. Table 5 gives, at different a values, the numbers of low branched chains in the three-dimensional models in excess of those calculated for the R(SU) model with the same a value, the shortfalls in the sums of the medium branched chains, as well as the excess of numbers of highly branched B chains. The range of B chain branching types over which the differences occurred are also given. The differences, as a percentage of the total numbers of chains in the branching type, are presented for the low and medium types. The fractions of A chains produced for a particular pair of extension

Table 5
Differences between three-dimensional and R(SU) models (number of chains per 1000)

Model and Z limit	a	Low branching[a]		Medium branching			High branching[b] 3D-R(SU)
		3D-R(SU) (s.e.)	3D-R(SU)/3D (%)	3D-R(SU)	Type of chains	3D-R(SU)/3D (%)	
3D(R)	0.35	−3 (6.4)	−0.7	+4	B_{2-5}	+1.4	−1
($Z = 60$)	0.43	−1 (2.6)	+0.2	−2	B_{2-5}	−0.6	0
	0.48	0 (4.6)	0	+1	B_{2-5}	+0.2	+1
	0.53	+6 (3.6)	+2.8	−8	B_{2-5}	−3.5	+2
	0.56	+14 (3.7)	+5.5	−10	B_{2-5}	−9.7	+4
	0.60	+12 (3.6)	+7.1	−17	B_{2-5}	−8.4	+4
	0.63	+14 (2.6)	+9.6	−20	B_{2-5}	−11.6	+6
3D(P)	0.37	−1 (4.2)	−0.2	+1	B_{2-5}	+0.5	+0.2
($Z = 60$)	0.44	+4 (4.4)	+1.2	−4	B_{2-5}	−1.5	+0.3
	0.50	+8 (3.1)	+3.2	−10	B_{2-5}	−4.5	+2
	0.55	+8 (5.2)	+3.7	−10	B_{2-5}	−4.7	+3
	0.61	+14 (5.7)	+8.1	−20	B_{2-6}	−9.9	+5
	0.65	+16 (3.2)	+11.4	−22	B_{2-7}	−11.5	+6
3D(R)	0.43	+8 (6.2)	+1.9	−12	B_{2-4}	−5.7	+2
($Z = 3$)	0.46	+17 (5.3)	+5.5	−23	B_{2-4}	−11.4	+6
	0.50	+30 (3.4)	+10.6	−41	B_{2-4}	−22.8	+11
	0.53	+40 (4.3)	+15.4	−52	B_{2-5}	−29.2	+12
	0.55	+49 (4.4)	+19.6	−62	B_{2-5}	−38.1	+13
	0.57	+52 (4.6)	+23.7	−65	B_{2-6}	−43.3	+12
	0.58	+58 (5.5)	+25.2	−72	B_{2-7}	−44.9	+14
3D(P)	0.42	+9 (3.2)	+2.0	−10	B_{2-5}	−3.4	+1
($Z = 3$)	0.49	+17 (6.1)	+6.1	−17	B_{2-5}	−8.0	+2
	0.54	+24 (7.4)	+10.4	−30	B_{2-5}	−15.2	+6
	0.59	+36 (7.1)	+17.9	−46	B_{2-6}	−25.5	+9
	0.63	+39 (3.4)	+21.9	−49	B_{2-8}	−27.7	+11
	0.67	+44 (4.8)	+28.2	−53	B_{2-8}	−33.2	+9

[a] Chain type, all B_1.
[b] Chain types, all chains > maximum medium chain type.

probabilities differed from those of the R(SU) model for all three-dimensional constructs and volume limits. Fig. 4 shows the relationship between E_B and a (at $B_A = B_B = 2$) for the four types of three-dimensional constructs—3D(R) and 3D(P) with the Z co-ordinate limits set at either $Z = +60$ to -60 or from $+3$ to -3. In comparison with the R(SU) model all the three-dimensional constructs, up to $E_B = 0.6$ had more A chains, and, apart from 3D(R) ($Z = \pm 3$) this persisted to higher E_B probabilities. It became lower for 3D(R) ($Z = \pm 3$) above $E_B = 0.7$. Both 3D(P) models were higher until a was 0.9. Among the three-dimensional models at a particular E_B, when this was low (0.05–0.10) a increased in the order 3D(R) ($Z = \pm 60$); 3D(P) ($Z = \pm 60$); 3D(P) ($Z = \pm 3$); 3D(R) ($Z = \pm 3$). For three of the models this relationship was maintained until $E_B = 0.7$ but the 3D(R) ($Z = \pm 3$) model was lower than 3D(P) ($Z = \pm 3$) at $E_B = 0.3$ and lower than all other models when $E_B \geq 0.5$.

When constructs were generated by the 3D(R) program, with a volume limit for Z set at $+60$ to -60 grid units and with E_B from 0.05 to 0.95 ($E_A = 1 - E_B$) and B_A and $B_B = 2$, at a values of 0.4–0.5 (Table 5) the numbers of B chains with each degree of branching were not significantly different from those of the R(SU) model with the same a value and, within a 3D(R) construct, the three axial radii were similar. Below $a = 0.68$ the mean of x was 12.2 (s.d. 0.81) of y 12.4 (s.d. 0.83) and of z 12.2 (s.d. 0.88). These indicate that with $T = 1260$, at all probabilities of extension, limits to X–Y and Z of ± 60 grid units gave no impediment to an increase in volume in any direction. From $a = 0.68$ to 0.82 the radii increased but was still well below 60, and the axial ratios remained near one. Thus, at $a$values near that of mammalian glycogen (0.42) with non-limiting extension of volume—leading to a spheroidal shape like that of glycogen—the numbers of B chains with different degrees of branching are similar in the 3D(R) model to those in the R(SU). Convolved plots of both 3D(R) ($Z = \pm 60$) and 3D(P) ($Z = \pm 60$), with the same chain length constants (ECL and ICL) and a as mammalian glycogen, resemble the chromatographic elution profiles of debranched chains versus d.p. of glycogen. All three fit the formula for the number of B_k chains as Tb^2a^{k-1} (where k is the number of branches) indicating that steric restriction is not a factor in the distribution between different types of B chains in glycogen.

From a values of 0.53–0.63 the number of B_1 chains (low branching chains) was higher in the 3D(R) ($Z = \pm 60$) than in the R(SU) model with the same a value—significantly at

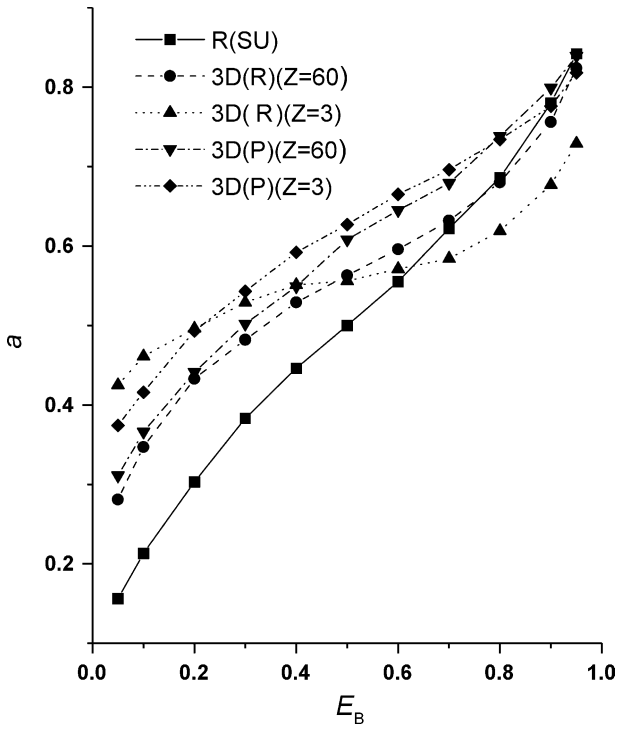

Fig. 4. a Values generated at different E_B probabilities for the R(SU) and various three-dimensional models.

$a = 0.56$ and 0.63 (Table 5). This positive difference was followed by a sequence of negative differences for the series of B chains with 2–5 branches (medium branched chains). At higher a values (≥ 0.68) the low branching chains extended to B_2 and at ≥ 0.82 to B_3. Then the sequence of negative differences extended to more highly branched chains (B_{3-7} at $a = 0.68$ and B_{4-13} at $a = 0.82$). This sequence of negative differences in medium branched chains was always followed by a sequence of positive differences of chains with more branches (highly branched chains). These tri-modal patterns of alternating positive and negative differences resemble those found for the differences between the experimental chromatographic profiles of numbers of chains versus d.p. for amylopectins and the convolved profiles calculated for R(SU) models (Table 3, Fig. 1). When the differences of the low and medium branched chains were calculated as percentages of the total numbers of the type of chain, these could be fitted with high correlation ($P < 0.0001$) to linear plots of percentages against a (Table 6). At low branching they increased as a increased and at medium branching became more negative. Another difference was an increase in the numbers of chains with high branching. This effect appears at $a \cong 0.5$. The differences are small and considerably less than those found for the differences between the experimental profiles and the convolved curves of the R(SU) models (Table 3). However, the absolute values of the medium branching differences were higher than the low branching values.

When preferential directions for branching were introduced (Table 1)—the 3D(P) ($Z = \pm 60$) model—the products became more ellipsoidal with a mean axial ratio $[(x + y)/2z]$ from $a = 0.31$ to 0.79 (11 readings) of 2.5 (s.d. 0.65). This is probably due to the preference for directing new chains into the X–Y plane. The differences from the R(SU) models with the same a value in the numbers of low, medium and high branching chains showed similar patterns to the 3D(R) ($Z = \pm 60$) model (Tables 5 and 6). When a was near that of mammalian glycogen the chain numbers were similar but as a increased above 0.5 increasing positive and negative differences for low and medium branching chains appeared. Differences for high branching chains were also positive. The differences of low and medium branching chains (as percentages) versus a could be fitted to linear plots with high correlation ($P < 0.0001$, Table 6) and with somewhat similar rates of change to those of the 3D(R) ($Z = \pm 60$) model. However, the total of differences of chain numbers (in absolute values) to the R(SU) models were much lower for these (with all the axial limits to

Table 6
Relationship between differences—3D minus R(SU)—in chain types (low, medium, high) as percentages of their totals, and a

Model	Branching chain type	Change in 3D-R(SU)/3D (%) with a	r	s.d.	Range of a values
3D(R) ($Z = 60$)	Low	$28a - 11$	0.92*	2.0	0.28–0.82
	Medium	$-47a + 19$	−0.95*	2.8	
3D(P) ($Z = 60$)	Low	$44a - 17$	0.92*	1.0	0.43–0.73
	Medium	$-47a + 18$	−0.95*	2.7	
3D(R) ($Z = 3$)	Low	$156a - 66$	0.997*	1.2	0.31–0.80
	Medium	$-232a + 92$	−0.95*	2.6	
3D(P) ($Z = 3$)	Low	$131a - 56$	0.98*	4.4	0.37–0.82
	Medium	$-150a + 62$	−0.99*	3.8	

*$P < 0.0001$; number of readings = 11.

Table 7
Highest degree of branching of B chains and, in brackets, no. of chains with > 14 branches

a	Model type		a	Model type	
	3D(R) ($Z = 60$)	R(SU)		3D(P) ($Z = 60$)	R(SU)
0.28	6	6	0.37	8	8
0.43	8	9	0.44	9	9
0.48	8	9	0.50	11	10
0.53	11	11	0.55	11	11
0.56	12	11	0.61	13	13
0.60	13	12	0.68	> 14(4)	> 14(2)
0.68	> 14 (4)	> 14(2)	0.74	> 14(9)	> 14(4)
0.82	> 14 (19)	> 14(14)	0.79	> 14(15)	> 14(10)
	3D(R) ($Z = 3$)	R(SU)		3D(P) ($Z = 3$)	R(SU)
0.43	9	9	0.37	8	8
0.46	10	9	0.42	8	9
0.50	11	10	0.49	10	10
0.53	14	11	0.54	13	11
0.55	> 14(1)	11	0.59	> 14(2)	12
0.57	> 14(5)	12	0.67	> 14(7)	> 14(1)
0.62	> 14(9)	13	0.73	> 14(17)	> 14(4)
0.73	> 14(18)	> 14(4)	0.82	> 14(28)	> 14(14)

volume set at 60 grid units) than between debranched amylopectins and the R(SU) models (Table 3). For *n*-maize amylopectin this total was 104 per 1000 chains, whereas for the 3D(R) ($Z = \pm 60$) model with $a = 0.56$ and the 3D(P) ($Z = \pm 60$) model with $a = 0.55$ they were 28 and 21, respectively. When co-ordinates of the volume limit in the Z direction were reduced to + 3 to − 3, giving a shape similar to the oblate ellipsoid that has been proposed for amylopectin, these totals of differences became more like those between experimental chromatograms and the R(SU) model. Both the 3D(R) ($Z = \pm 3$) and 3D(P) ($Z = \pm 3$) models had tri-modal patterns of differences from R(SU) models of positive, negative and positive (Table 5). However, the rates of change (Table 6) were much higher than for the three-dimensional models with all axial limits set to 60, and the sums of the absolute numbers of total chain differences were of the same order as the differences between the experimental chromatograms and convolved curves of R(SU) constructs. With the 3D(R) ($Z = \pm 3$) model, when a was 0.55 and 0.57, these were 124 and 129 chains, and with 3D(P) ($Z = \pm 3$) at 0.54 and 0.59, 60 and 91. With the volume limit set in the Z direction at ± 3 units, the radius of the $X-Y$ plane increased considerably. In the 3D(R) ($Z = \pm 3$) model from $a = 0.46$ to 0.57 the radius was approximately 23 grid units and in the 3D(P) ($Z = \pm 3$) somewhat higher; from $a = 0.42$ to 0.67 approximately 28 grid units. The differences of chain numbers were less marked in the 3D(P) than in the 3D(R) model. This may be a consequence of directing new chains in the 3D(P) model into the $X-Y$ plane, giving a higher $X-Y$ radius.

The three-dimensional models differ from the R(SU) models in another way. For both the 3D(R) and 3D(P) with a volume limit of $Z = \pm 3$, as the content of A chains increased the numbers of B chains with more branches increased relative to the R(SU) model with the same a value (Table 7). In the 3D(R) ($Z = \pm 3$) model with an a value of 0.55 there was 1 chain with > 14 branches, whereas in the R(SU) model the maximum degree of branching was 11. This greater number of more highly branched chains in the three-dimensional models was linked to the presence of more longer chains. In an R(SU) model with an a value of 0.56 ($T = 1260$, $B_A = B_B = 2$) there were 4 chains > 13 grid units; whereas in the 3D(R) and 3D(P) models there were 16 and 14. These longer chains could serve as links between clusters. On the other hand, when the fraction of A chains was near that of mammalian glycogen (0.42) the chains in the R(SU), 3D(R) and 3D(P) models all had maximum lengths of 11 grid units.

Fig. 5 compares convolved graphs of weight of glucan versus d.p. of 3D(R) ($Z = \pm 3$) and 3D(P) ($Z = \pm 3$) with the R(SU) models with the same A chain content. In Fig. 5A,

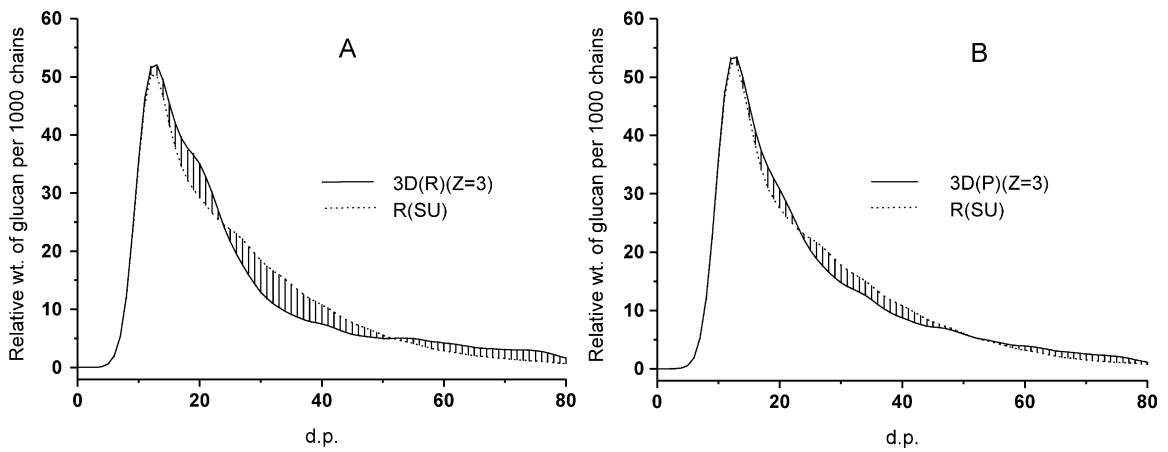

Fig. 5. Comparisons of convolved profiles of weight of glucan of R(SU) and three-dimensional ($Z = 3$) models with similar CL, ICL and a values. R(SU) (- - -) and 3D(R) (—) models (A); ICL = 6, ECL = 12 ($ECL_B = CL_{A)}$ $a = 0.55$ convolved as $T = 1260$; A chains, 216 at d.p. 10.8, $w = 4$; 477 at 12.8, $w = 6$; B chains at $w = 7$. R(SU) (– – -) and 3D(P) (—) models (B); ICL = 6, ECL = 12 ($ECL_B = CL_{A)}$ $a = 0.57$ convolved as $T = 1260$; A chains, 237 at d.p.10.8, $w = 4$; 514 at 12.8, $w = 6$; B chains at $w = 7$.

relative weight per 1000 versus d.p. of a 3D(R) model (with $a = 0.55$, ECL = 12 and ICL = 6 and assuming $ECL_B \approx CL_A$) and the R(SU) model with the same constants are compared. In Fig. 5B, this comparison has been made for the 3D(P) model with $a = 0.57$ and similar average chain lengths. They both show the alternating tri-modal (positive, negative, positive) pattern characteristic of comparisons of chromatograms of debranched amylopectins with the R(SU) model with the same A chain content and average chain lengths (Fig. 1, Table 3).

The architecture of the mammalian glycogen molecule differs from that of amylopectin in several ways. As well as lower measurements for the various chain lengths, the axial ratio indicates a spheroidal shape: amylopectin is an oblate ellipsoid. F is 1.7 compared to 2.2 for n-maize (Yun et al., 1993). The fraction of glucan in core chains is greater (Matheson, 1996). The three-dimensional models generated with non-limited expansion in any direction, with an a value near 0.42 gave a spheroidal shape, whose convolved plot of numbers of chains versus d.p.—calculated with the average chain lengths of glycogen—resembles that of mammalian glycogen, which has a spheroidal shape. As well, the profile of α(1–4) chains of mammalian glycogen is similar to that of a convolved plot of the R(SU) model with the same constants (Matheson et al., 1999). This suggests that, at this lower content of A chains and without limit to expansion in any direction, the mammalian glycogen chain distribution between B chains is not affected by steric restriction, giving fractions fraction of B chains with k branches of approximately b^2a^{k-1}.

In three-dimensional models with an a value near that of amylopectin, in particular those with limited expansion in one direction [3D(R) ($Z = \pm 3$) and 3D(P) ($Z = \pm 3$)] the differences between their convolved plots and those of the R(SU) model with the same a value and average chain lengths are similar to those between the experimental chromatographic profile of a debranched amylopectin and the R(SU) model: they show an alternating tri-modal pattern (positive, negative, positive). In the three-dimensional ($Z = \pm 3$) models, there are increased numbers of chains with more branches, and also of longer chains, than in the equivalent R(SU) model. Longer chains than in the R(SU) model are found in amylopectin. These three-dimensional ($Z = \pm 3$) models have an oblate ellipsoidal shape similar to amylopectin,. With their limit to expansion in one direction and steric restrictions to chain placement in three-dimensional space, producing a tri-modal pattern of difference of chain numbers versus d.p., they indicate a possible model for the distribution between α(1–4) chains in amylopectin. Ultimately structural aspects of α(1–4)(1–6) glucans need to be related to the actions of the biosynthetic enzymes, including the role of debranching activity (Manners, 1997; Myers, Morell, Ball, & James, 2000) and the more recent observation of extension of α(1–4) chains at the reducing end in amylopectin synthesis (Mukerjea, Yu, & Robyt, 2002).

References

Ahmad, F. B., Williams, P. A., Doublier, J.-L., Durand, S., & Buleon, A. (1999). Physico-chemical characterisation of sago starch. *Carbohydrate Polymers*, *38*, 361–370.

Baba, T., & Arai, Y. (1984). Structural characterisation of amylopectin and intermediate material in amylomaize starch granules. *Agricultural Biological Chemistry*, *48*, 1763–1775.

Baba, T., Uemura, R., Hiroto, M., & Arai, Y. (1987A). Structural features of amylomaize starch components of amylon 50 starch. *Journal of Japanese Society Starch Science*, *34*, 196–202.

Baba, T., Uemura, R., Hiroto, M., & Arai, Y. (1987B). Structural features of amylomaize starch components of amylon 70 starch. *Journal of Japanese Society Starch Science*, *34*, 213–217.

Banks, W., Geddes, R., Greenwood, C. T., & Jones, I. G. (1972). The molecular size and shape of amylopectin. *Starch*, *24*, 245–251.

Bertoft, E. (1989). Investigation of the fine structure of amylopectin using alpha- and beta-amylase. *Carbohydrate Research*, *189*, 195–207.

Bertoft, E., & Koch, K. (2000). Composition of chains in waxy-rice starch and its structural units. *Carbohydrate Polymers*, *41*, 121–132.

Boyer, C. D., Damewood, P. A., & Matters, G. L. (1980). Effect of gene dosage of high amylose loci on the properties of the amylopectin fractions of the starches. *Starch*, *32*, 217–222.

Bryce, W. A. J., Cowie, J. M. G., & Greenwood, C. T. (1957). The sedimentation behaviour of the components of potato starch in dilute alkali. *Journal Polymer Science*, *25*, 251–253.

Bullen, K. E. (1962). *An introduction to the theory of mechanics*. Sydney: Science Press, p. 181.

Burchard, W., & Thurn, A. (1985). Heterogeneity in branching. Mathematical treatment of the amylopectin structure. *Macromolecules*, *18*, 2072–2082.

Callaghan, P. T., & Lelievre, J. (1985). The size and shape of amylopectin:a study using pulsed-field gradient nuclear magnetic resonance. *Biopolymers*, *24*, 441–460.

Callaghan, P. T., & Lelievre, J. (1986). The influence of polymer size and shape on self-diffusion of polysaccharides and solvents. *Analytica Chimica Acta*, *189*, 145–166.

Callaghan, P. T., Lelievre, J., & Lewis, J. A. (1987). A comparison of the size and shape of β-limit dextrin and amylopectin using pulsed field-gradient nuclear magnetic resonance and analytical ultracentrifugation. *Carbohydrate Research*, *162*, 33–40.

Durrani, C. M., & Donald, A. M. (2000). Shape, molecular weight distribution and viscosity of amylopectin in dilute solution. *Carbohydrate Polymers*, *41*, 207–217.

Ebermann, R., & Schwarz, R. (1975). Fractionation of starch by gel filtration on agarose beads. *Starch*, *27*, 361–363.

French, D. (1984). Organization of starch granules. In R. L. Whistler, J. N. BeMillar, & E. E. Paschall (Eds.), *Starch chemistry and technology* (2nd edition) (pp. 183–247). Orlando: Academic Press.

Gérard, C., Barron, C., Colonna, P., & Planchot, V. (2001). Amylose determination in genetically modified starches. *Carbohydrate Polymers*, *44*, 19–27.

Gérard, C., Colonna, P., Buléon, A., & Planchot, V. (2002). Order in maize mutant starches revealed by mild acid hydrolysis. *Carbohydrate Polymers*, *48*, 131–141.

Greenwood, C. T., & Robertson, J. S. M. (1954). Physico-chemical studies on starches. Part 1. The characterisation of the starch present in the seeds of the rubber tree, *Hevea brasiliensis*. *Journal of Chemical Society*, 3769–3778.

Gunja-Smith, Z., Marshall, J. J., Mercier, C., Smith, E. E., & Whelan, W. J. (1970). A revision of the Meyer–Bernfeld model of glycogen and amylopectin. *FEBS Letters*, *12*, 101–104.

Hanashiro, I., Abe, J.-I., & Hizukuri, S. (1996). A periodic distribution of the chain length of amylopectin as revealed by high-performance anion-exchange chromatography. *Carbohydrate Research*, *283*, 151–159.

Hizukuri, S. (1986). Polymodal distribution of the chain lengths of amylopectins, and its significance. *Carbohydrate Research*, *147*, 342–347.

Jane, J., Chen, Y. Y., Lee, L. F., McPherson, A. E., Wong, K. S., Radosalvjevic, M., & Kasemsuwan, T. (1999). Effects of amylopectin branch chain length and amylose content on the pasting properties of starch. *Cereal Chemistry*, *76*, 629–637.

Kerr, R. W. (1945). The heterogeneity of amylose and amylopectin, part 1. *Archives of Biochemistry*, *7*, 377–392.

Klingler, R. W., & Zimbalski, M. (1992). Molekulare charakterisierung von amylosen verschiedenen Ursprungs. *Starch*, *44*, 414–418.

Klucinec, J. D., & Thompson, D. B. (1998). Fractionation of high-amylose maize starches by differential alcohol precipitation and chromatography of the fractions. *Cereal Chemistry*, *75*, 887–896.

Larner, J., Ray, B. R., & Crandall, H. F. (1956). Pattern of action of crystalline muscle phosphorylase on glycogen as determined from molecular size distribution studies. *Journal American Chemical Society*, *78*, 5890–5898.

Lelievre, J., Lewis, J. A., & Marsden, K. (1986). The size and shape of amylopectin: a study using analytical ultracentrifugation. *Carbohydrate Research*, *153*, 195–203.

MacGregor, A. W., & Morgan, J. E. (1984). Structure of amylopectins isolated from large and small starch granules of normal and waxy barley. *Cereal Chemistry*, *61*, 222–228.

McPherson, A. E., & Jane, J. (1999). Comparison of waxy potato with other root and tuber starches. *Carbohydrate Polymers*, *40*, 57–70.

Madsen, N. B., & Cori, C. F. (1958). The binding of glycogen and phosphorylase. *Journal of Biological Chemistry*, *233*, 1251–1256.

Manners, D. J. (1989). Recent developments in our understanding of amylopectin structure. *Carbohydrate Polymers*, *11*, 87–112.

Manners, D. J. (1997). Observations on the possible involvement of debranching enzymes in starch biosynthesis. *Journal of Applied Glycoscience*, *44*, 541–546.

Manners, D. J., & Matheson, N. K. (1981). The fine structure of amylopectin. *Carbohydrate Research*, *90*, 99–110.

Matheson, N. K. (1971). Amylose changes in the starch of developing wheat grains. *Phytochemistry*, *10*, 3213–3219.

Matheson, N. K. (1975). The α(1–4)(1–6) glucans from sweet and normal corns. *Phytochemistry*, *14*, 2017–2021.

Matheson, N. K. (1990). A comparison of the structure of normal and high amylose pea-seed starches prepared by precipitation with concanavalin A. *Carbohydrate Research*, *199*, 195–205.

Matheson, N. K. (1996). The chemical structure of amylose and amylopectin fractions of starch from tobacco leaves during development and diurnally–nocturnally. *Carbohydrate Research*, *282*, 247–262.

Matheson, N. K., & Caldwell, R. A. (1999). α(1–4)Glucan chain disposition in models of α(1–4)(1–6)glucans: comparison with structural data for mammalian glycogen and waxy amylopectin. *Carbohydrate Polymers*, *40*, 191–209.

Matheson, N. K., & Welsh, L. A. (1988). Estimation and fractionation of the essentially unbranched (amylose) and branched (amylopectin) components of starches with concanavalin A. *Carbohydrate Research*, *180*, 301–313.

Millard, M. M., Wolf, W. J., Dintzis, F. R., & Willett, J. L. (1999). The hydrodynamic characterization of waxy maize amylopectin in 90% dimethyl sulfoxide-water by analytical ultracentrifugation, dynamic and static light scattering. *Carbohydrate Polymers*, *39*, 315–320.

Mukerjea, R., Yu, L., & Robyt, J. F. (2002). Starch biosynthesis: mechanism for the elongationof starch chains. *Carbohydrate Research*, *337*, 1015–1022.

Myers, A. M., Morell, M. K., James, M. G., & Ball, S. G. (2000). Recent progress toward understanding biosynthesis of the amylopectin crystal. *Plant Physiology*, *122*, 989–997.

Nikuni, Z. (1978). Studies on starch granules. *Starch*, *30*, 105–111.

Oates, C. G. (1990). Fine structure of mung bean starch: an improved method of fractionation. *Starch*, *42*, 464–467.

O'Shea, M. G., & Morell, M. K. (1996). High resolution slab gel electrophoresis of 8-amino-1, 2, 6-pyrenetrisulfonic acid (APTS) tagged oligosaccharides using a DNA sequencer. *Electrophoresis*, *17*, 681–686.

Robin, J. P., Mercier, C., Charbonniere, R., & Guilbot, A. (1974). Gel filtration and enzymatic studies of insoluble residues from prolonged acid treatment of potato starch. *Cereal Chemistry*, *51*, 389–406.

Shibanuma, Y., Takeda, Y., & Hizukuri, S. (1996). Molecular and pasting properties of some wheat starches. *Carbohydrate Polymers*, *29*, 253–261.

Song, Y., & Jane, J. (2000). Characterisation of barley starches of waxy, normal, and high amylose varieties. *Carbohydrate Polymers*, *41*, 365–377.

Takeda, Y., Hizukuri, S., & Juliano, B. O. (1986). Purification and structure of amylose from rice starch. *Carbohydrate Research*, *148*, 299–308.

Tao, L., & Matheson, N. K. (1993). The role of the structure on the molecular size and conformation of (1–4) and (1–6) linked polysaccharides. *Carbohydrate Polymers*, *20*, 269–277.

Thompson, D. B. (2000). On the non-random nature of amylopectin branching. *Carbohydrate Polymers*, *43*, 223–239.

Thorn, W., & Mohazzeb, S. (1990). Molecular weights, lengths, and distributions of side chains in α-D-polyglucans. *Starch*, *42*, 373–376.

Whistler, R. L., & Doane, W. M. (1961). Characterisation of intermediate fractions of high-amylose corn starches. *Cereal Chemistry*, *38*, 251–255.

Wong, K. S., & Jane, J. (1997). Quantitative analysis of debranched amylopectin by HPAEC-PAD with a post-column enzyme reactor. *Journal of Liquid Chromatography and Related Technology*, *20*, 297–310.

Yamada, T., & Taki, M. (1976). Fractionation of maize starch by gel-chromatography. *Starch*, *28*, 374–377.

Yeh, J. Y., Garwood, D. L., & Shannon, J. C. (1981). Characterisation of starch from maize endosperm mutants. *Starch*, *33*, 222–230.

Yun, S.-H., & Matheson, N. K. (1992). Structural changes during development in the amylose and amylopectin fractions (separated by precipitation with concanavalin A) of starches from maize genotypes. *Carbohydrate Research*, *227*, 85–101.

Yun, S.-H., & Matheson, N. K. (1993). Structures of the amylopectins of waxy, normal, amylose-extender and *wx* : *ae* genotypes, and of phytoglycogen of maize. *Carbohydrate Research*, *243*, 307–321.